Applied Thermal Engineering 123 (2017) 753–760

Contents lists available at ScienceDirect

Applied Thermal Engineering

journal homepage: www.elsevier.com/locate/apthermeng

Research Paper

# Consolidated adsorbent containing graphite flakes for heat-driven water sorption cooling systems

Khorshid Fayazmanesh, Claire McCague, Majid Bahrami *

*Laboratory for Alternative Energy Conversion (LAEC), School of Mechatronic Systems Engineering, Simon Fraser University, 250-13450 102 Avenue, Surrey, BC V3T 0A3, Canada*

## HIGHLIGHTS

- New composite adsorbents were prepared by consolidating graphite flakes with silica gel using binders with different molecular weights.
- The 40,000 MW PVP binder had substantially less effect on the pore volume, pore size distribution and water uptake of silica gel-$CaCl_2$ composites than the 10,000 MW PVP binder.
- The water uptake of the silica gel-$CaCl_2$-PVP40 composite was consistent through 300 pressure swing cycles.
- The thermal conductivity of a set of S6-$CaCl_2$-PVP40 sorbent with 0–20 wt% graphite flakes were tested at 2 and 20 RH%.
- The effect of thermally conductive additives on water uptake and thermal conductivity studied.

## ARTICLE INFO

*Article history:*
Received 16 March 2017
Revised 19 May 2017
Accepted 21 May 2017
Available online 25 May 2017

*Keywords:*
Sorption chiller
Consolidated adsorbent
Water sorption
Thermal conductivity
Graphite flakes

## ABSTRACT

Thermally-driven sorption cooling systems can reduce the primary energy demand for air conditioning and refrigeration. The specific cooling performance (SCP) of an adsorption cooling system can be enhanced by increasing the heat transfer rate in a heat exchanger packed or coated with sorbent material. In this study, calcium chloride in a silica gel matrix was combined with a binder and graphite flakes to produce water absorbent consolidated composites. The characteristics of the composites were evaluated by porosimetry and transient plane source (TPS) thermal properties analysis. The addition of 20 wt% graphite flakes increased the thermal conductivity of the composite adsorbent from 0.57 W $m^{-1}$ $K^{-1}$ to 0.78 W $m^{-1}$ $K^{-1}$. Water sorption isotherms and vapor pressure swing durability tests were collected with a thermogravimetric vapor sorption analyser. Water uptake capacity of samples at a 1.2 kPa vapor pressure decreased from 0.32 g/g for $CaCl_2$/silica gel to 0.15 g/g for silica gel/$CaCl_2$ consolidated with 10 wt% graphite flakes and 13 wt% binder. Water sorption during vapor pressure durability test was consistent within 28.5 and 18 wt% across 150 cycles at 25 and 35 °C.



## 1. Introduction

In the early 1900s, ammonia-$CaCl_2$ and methanol-activated carbon absorption cooling systems were developed and commercialized for industrial and residential refrigeration [1,2]; and mobile freezer systems with $SO_2$-silica gel as the adsorbate-adsorbent working pair were developed for the transportation of frozen fish by rail [3]. Shortly thereafter, cost effective vapor-compression cycle refrigeration systems using toxic refrigerants and electrical motors conquered the commercial market and sorption cooling systems disappeared for over 60 years [4]. This development stagnation lasted until the environmental costs of air conditioning and refrigeration, including the depletion of the ozone layer, the energy consumption of compressors, and the role of greenhouse gas emissions (hydrofluorocarbon refrigerants and $CO_2$) in climate change became a concern [4]. One of the sustainable and clean solutions for thermal management and heat storage is heat-driven sorption technology [5,6]. Sorption-cooling systems utilize environmentally friendly refrigerants, such as water, and can generate cooling power from low-grade industrial waste heat or renewable thermal energy sources (solar or geothermal).

The majority of commercial adsorption cooling systems use a granular adsorbent packed in a finned-tube heat exchanger [5,7,6]. However, the high contact thermal resistance between granules and the heat exchanger surface remains a major challenge [8]. Several methods to improve heat transfer have been investigated, such as synthesizing adsorbent on the heat exchanger surface [6], consolidating sorbents by compacting them with thermally conductive materials into a solid matrix [9], and coating

* Corresponding author.
*E-mail address:* mbahrami@sfu.ca (M. Bahrami).

http://dx.doi.org/10.1016/j.applthermaleng.2017.05.114
1359-4311/

**Nomenclature**

| | | | |
|---|---|---|---|
| LDF | Linear Driving Force | t | time (LDF model) |
| BET | Brunauer, Emmett and Teller model | $\tau$ | characteristic time (s) |
| BJH | Barrett, Joyner and Halenda model | $S$ | specific surface area ($m^2\ g^{-1}$) |
| RH | Relative Humidity | $V$ | pore volume ($cm^3\ g^{-1}$) |
| SCP | specific cooling performance ($W\ g^{-1}$) | u(t) | water sorption at time t |
| TPS | transient plane source | $\Delta u$ | total change in uptake |
| $D$ | average pore diameter (nm) | $w$ | water uptake (g/g of sorbent) |
| $h_{fg}$ | water enthalpy of evaporation ($kJ\ kg^{-1}$) | $\Delta\omega$ | total weight change (g/g of sorbent) |
| k | time constant | | |

a heat exchanger surface with a composite adsorbent [5]. The first two methods improve heat transfer performance, but can decrease water uptake rate [10]. For coatings with composite adsorbents, the main issue is choosing a binder composition and concentration without blocking pores.

Detail studies on hygroscopic salts confined to a porous host matrix have been done for sorption systems at the Boreskov Institute of Catalysis and ITAE/SNR in Messina, Italy [11]. Ponomarenko et al. prepared $CaCl_2$ confined in SBA-15 silica gel with water sorption capacity of 0.47 g/g at 50 °C and water vapor $P/P_0 < 0.3$ [12]. Temperature swing water sorption tests (60–30 °C) with vapor pressure of 1.23 kPa have been performed to compare CaCl2/SBA (mesoporous silica gel, average pore diameter 11.8 nm) with microporous silica gel (Fuji RD) under sorption system operating conditions. The $CaCl_2$/SBA has over twice the specific cooling power calculated from the measured sorption rate [13]. SWS-1L ($CaCl_2$ in mesoporous silica gel) demonstrated the coefficient of performance (COP) 0.6 at desorption as low as 85–95 °C in compare to silica gel-water and zeolite-water systems at low temperature heat generation [14]. Freni et al. provided a detailed comparative study on the most promising working pairs for thermal driven adsorptive heat pump, air conditioning and refrigeration applications [15]. For air conditioning and pumping purposes working with water as adsorbate, the highest heating/cooling COP up to 1.62/0.71 is reported for AQSOA-FAM Z02, LiBr-Silica gel and $CaCl_2$-Silica gel [15].

The thermal conductivity of sorbents has a great impact on the dynamic performance of the sorption systems. Tanashev et al. showed that the thermal conductivity of $CaCl_2$/silica gel KSK increased from 0.13 $W\ m^{-1}\ K^{-1}$ to 0.5 $W\ m^{-1}\ K^{-1}$ as absorbed water content increased from 0.1 g/g to 0.8 g/g [16]. Heat transfer enhancement can be also achieved by binding or synthesizing adsorbent on the surface of the adsorber bed [17,18] or by physically mixing sorbents with materials with higher thermal conductivity, such as metal powders or synthetic graphite [19]. Restuccia et al. observed that the thermal conductivity of zeolite with 40 wt% aluminum hydroxide, 0.43 $W\ m^{-1}\ K^{-1}$, was greater than the thermal conductivity of zeolite with 40 wt% graphite or 40 wt% PTFE (polytetrafluoroethylene), 0.36 and 0.25 $W\ m^{-1}\ K^{-1}$, respectively [19]. Wu et al. synthesized a silica gel – copper nanopowder composite by a sol-gel process and measured the thermal conductivity by the transient plane source (TPS) method. Wu et al. found that the copper nanopowder enhanced the thermal conductivity by 20% to 0.19 $W\ m^{-1}\ K^{-1}$ [20]. Effective thermal conductivity of unconsolidated adsorbent improved from 0.106 $W\ m^{-1}\ K^{-1}$ to 0.363 $W\ m^{-1}\ K^{-1}$ by adding 15 wt% shaved aluminum [21]. Kim et al. fabricated silica gel composite mixed with expanded graphite powders by compressive molding method. The thermal conductivity of the composite blocks is reported 10–20 $W\ m^{-1}\ K^{-1}$ depending on the graphite bulk density [22,23]. Sorption heat pumps with composite materials can have higher specific cooling power and lower investment cost [19].

The specific cooling performance (SCP) can be improved by the development of new composite materials with high water uptake and increased heat and mass transfer properties. In this study, $CaCl_2$-silica gel was selected for its known strong water sorption properties. Composites were prepared with organic binders (polyvinylpyrrolidone) and thermally conductive additives. The surface area and pore size distribution were measured. Water uptake and multi-cycle performance of the samples at different temperatures were measured and the thermal conductivity of the composite adsorbents and a mixture of silica gel and graphite flakes (0–20 wt%) studied under different controlled relative humidity.

## 2. Experimental study

### 2.1. Sample preparation

Composite sorbents were prepared utilizing chromatography-grade commercial silica gel (SiliaFlash® B60, Lot 011112, Silicycle, Inc., Quebec, Canada) with 0.2–0.5 mm irregularly shaped grains and average pore diameter of 6 nm. In batches of 50 g, the dry mesoporous silica gel was wetted with ethanol. An aqueous solution containing $CaCl_2$ and either 10,000 MW polyvinylpyrrolidone (PVP10) binder (Sigma Aldrich) or 40,000 MW polyvinylpyrrolidone (PVP40) binder (Amresco) was added, and the slurry was dried in a fume hood for 24 h. The damp materials were oven dried at 180 °C for over 2 h. The composition and volume of solution added to the silica gel was such that the consolidated composite produced was 28 wt% $CaCl_2$ and 15 wt% PVP. Dry silica gel in 4 g batches was combined with PVP (12–15 wt%) and thermally conductive graphite flakes (150 μm, Sigma-Aldrich) or copper powder (<425 μm, Sigma-Aldrich). The graphite flakes added to the composite included both fine particles and thin flakes up to 1.3 mm long, while the copper particles were small (up to 0.41 mm). Consolidated composites with thickness of 3.6 mm were also prepared with and without $CaCl_2$. The slurries were baked for one hour at 50 °C until damp or dry, and then heated to 180 °C for one hour. The sample names and compositions of the sorbent composites are given in Table 1.

### 2.2. Characterization

Nitrogen sorption isotherms of the samples were collected with a volumetric physisorption analyser (ASAP 2020, Micromeritics Instruments) to determine the specific surface area ($S_{BET}$), average pore diameter ($D$) and pore volume ($V$). Prior to testing, the samples were dried under vacuum at 150 °C for 1 h, followed by 2 h

**Table 1**
Composites prepared with SiliaFlash B60 silica gel matrix.

| Sample name | Silica gel | $CaCl_2$ | PVP | Graphite flakes |
|---|---|---|---|---|
| S6-0%G | 4 g | – | – | – |
| S6-5%G | 4 g | – | – | 0.21 g |
| S6-10%G | 4 g | – | – | 0.44 g |
| S6-20%G | 4 g | – | – | 1 g |
| S6-$CaCl_2$-PVP10 | 50 g | 25 g | 20 g | – |
| S6-$CaCl_2$-PVP40 | 50 g | 25 g | 20 g | – |
| S6-PVP40-0%G | 4 g | – | 0.7 | – |
| S6-PVP40-5%G | 4 g | – | 0.7 | 0.24 |
| S6-PVP40-10%G | 4 g | – | 0.7 | 0.52 |
| S6-PVP40-20%G | 4 g | – | 0.7 | 1.175 |
| S6-$CaCl_2$-PVP40-0%G | 4 g | 1.71 g | 1 g | – |
| S6-$CaCl_2$-PVP40-5%G | 4 g | 1.71 g | 1 g | 0.35 g |
| S6-$CaCl_2$-PVP40-10%G | 4 g | 1.71 g | 1 g | 0.74 g |
| S6-$CaCl_2$-PVP40-20%G | 4 g | 1.71 g | 1 g | 1.67 g |
| | | | | Copper powder |
| S6-PVP40-0%C | 4 g | – | 0.7 | – |
| S6-PVP40-5%C | 4 g | – | 0.7 | 0.24 |
| S6-PVP40-10%C | 4 g | – | 0.7 | 0.52 |

at 200 °C. The $S_{BET}$ was calculated with the Brunauer, Emmett and Teller (BET) model while the Barrett, Joyner and Halenda (BJH) model was used to calculate the incremental pore volume from the adsorption curves [24,25]. The composite microstructure was imaged with a scanning electron microscope (FEI/Aspex-Explorer) at room temperature.

A transient plane source 'hot disk' thermal constants analyzer (TPS 2500S, ThermTest Inc., Fredericton, Canada) was used to measure the thermal conductivity of the samples (Fig. 1). The 'hot disk', a Kapton encapsulated double spiral nickel wire sensor (design #7577) with a 2 mm radius, is used for both transient heating of the sample and as precise resistance thermometer for simultaneous temperature measurements. The sensor is placed between a pair of identical samples. The roughness of the surfaces should be approximately smaller than the disk diameter about an order of magnitude. Constant temperature difference develops at the sample-sensor interfaces as a result of contact resistance between the sensor and sample surface. The effect of this constant temperature difference on the measured sample properties is de-convoluted in the calculations [26–28].

Tests were performed in a temperature and humidity controlled chamber. Humidity was monitored in the chamber and controlled by a humidifier (P-10C-1C-2-0-031300-v7, Cellkraft AB, Sweden) with a flow rate of 5 nominal litres per minute. The samples with the thickness of 3.5 mm in average were tested at 5%RH and 20%RH at 35 °C. The thermal conductivity of three different areas of each S6-$CaCl_2$-PVP40-G composite sample was tested five times under each condition; a standard deviation of 10% has been measured.

Water sorption isotherms (0–2.7 kPa) for the composite adsorbents were measured using a thermogravimetric vapor sorption analyzer (IGA-002, Hiden Isochema), shown in Fig. 2. Isotherms were collected at 35 and 78 °C. Prior to water sorption cycle tests, the samples were dried under vacuum for 6 h at 90 °C and the dry masses were recorded.

## 3. Result and discussion

### 3.1. Pore-size distribution

The differential pore volume distribution of the silica and composite samples were obtained through analysis of the adsorption branch of the $N_2$ isotherms and is shown in Fig. 3. As summarised in Table 2, the 28 wt% in S6-$CaCl_2$; 25.5 wt% (total) in S6-$CaCl_2$-PVP10 and PVP40 (30 wt% considering only $CaCl_2$ to S6) was distributed within the silica gel pores, decreasing the $S_{BET}$ and $V$, and increasing the average pore diameter from 4.8 to 7 nm. Comparing samples S6-$CaCl_2$-PVP10 and S6-$CaCl_2$-PVP40, the surface area and pore volume decreased significantly for the sample containing PVP10, the lower molecular weight binder. The SEM images

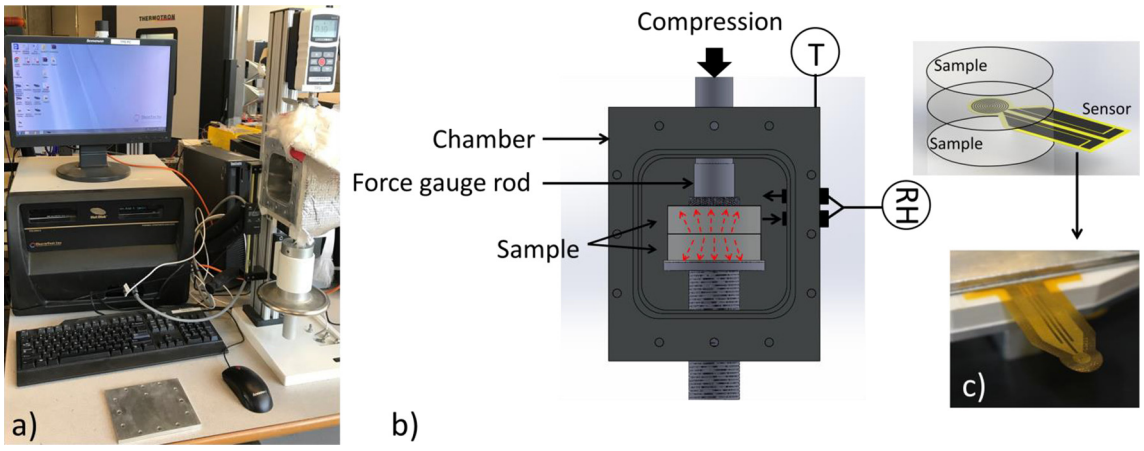


**Fig. 1.** (a) TPS thermal constants analyzer. (b) Schematic of TPS. (c) Double spiral "hot disk" nickel sensor.

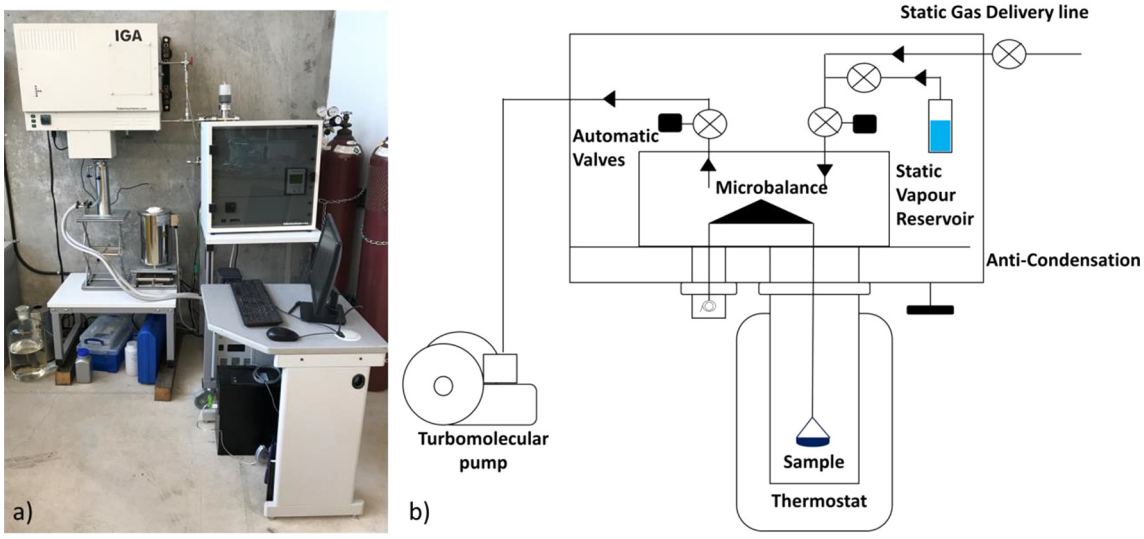


**Fig. 2.** (a) Thermogravimetric analyzer. (b) Schematic of thermogravimetric analyzer.

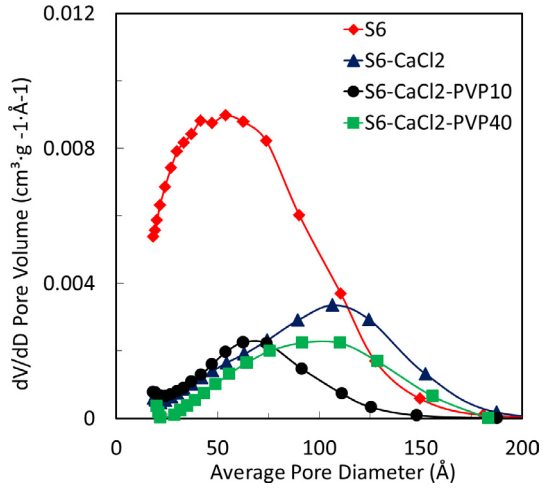


**Fig. 3.** Pore size distribution plots for silica gel and composites from $N_2$ adsorption isotherms fit with BJH model utilizing Hasley: FAAS statistical thickness curves.

of loose grain silica gel, S6, and S6-$CaCl_2$-PVP40 composite shown in Fig. 4, indicate that the binder does not fill the voids between silica gel particles. Fig. 3 shows random orientation of graphite flakes in the composite.

### 3.2. Water vapor sorption

The water sorption properties of sorbents with PVP10 and PVP40 binders were measured at 25, 35 and 78 °C, as shown in Fig. 5. Water uptake capacity, $w$, is calculated as $m_{water}/m_{dry\ sorbent}$, where the mass of the dry sorbent includes all ingredients (salt, porous matrix, binder, and thermally conductive additives). For S6-$CaCl_2$-PVP40, the water uptake at 34.7 °C and 2 kPa was 0.34 g/g while for S6-$CaCl_2$-PVP10 it was only 0.29 g/g. The greater infiltration of the pore structure by the lower molecular weight PVP10 (Table 3) has a negative impact on absorption.

The difference in equilibrium water content of the samples under operational cycle conditions for adsorption (1.2 kPa, 35 °C) and desorption (2.3 kPa, 80 °C) are summarised in Table 3. There was no loss in the water uptake capacity of the active materials in the sorbents containing 20 wt% binder. PVP is a hygroscopic binder with water uptake of up to 6.6 wt% at 1.2 kPa, 35 °C for the bulk material. In Fig. 6, water sorption isotherms (35 °C) for the composite samples are plotted in $mol_{H2O}$ per $mol_{CaCl2}$ the water uptake per mole of active material, the salt, indicates minimal variation in performance. However, the overall performance of sorbent material is reduced in proportion to the dead weight of additives.

The isosteric heat of water sorption is determined as a function of the slope of the linear isosters, where $\mathrm{Ln}(P) = B(w)/T + C(w)$ and $\Delta H_{is}(w) = B(w)R$ and $R$ is the universal gas constant. As $w$ approaches 0.1 g/g (shown in Fig. 7), the $\Delta H_{is}(w)$ reaches to −62.8 kJ/mol.

The kinetic curves were fitted with the linear driving force (LDF) model,

$$u(t) = \Delta u\left(1 - e^{-\frac{t}{k}}\right) \quad (1)$$

where $u(t)$ is uptake at time $t$, $k$ is time constant and $\Delta u$ is the total change in uptake [29]. The kinetic curves for 0.2 kPa steps to and 1.6–1.8 kPa at 35 °C are shown in Fig. 8 for samples with and without binder. The sorption relaxation coefficient of the samples at different low pressures (0.9, 1.2 and1.8 kPa) pressure are summarised in Table 4. The water sorption constant rate of loose grain S6-$CaCl_2$ is greater than S6-$CaCl_2$-PVP40 as a result of its surface area and total volume. Addition of binder reduces the gap between particles and vapor diffusion inside pores.

**Table 2**
Surface characteristics of silica gel and silica-supported $CaCl_2$ composites.

| Sample | $S_{BET}$ ($m^2\ g^{-1}$) | $V$ ($cm^3\ g^{-1}$) | $D$ (nm) | Product specifications $S_{BET}$, V, particle size |
|---|---|---|---|---|
| S6 | 494 | 0.77 | 4.8 | 514 $m^2$/g, 0.75 $cm^3$/g, 0.2–0.5 mm |
| S6-$CaCl_2$ | 134 | 0.31 | 7.0 | – |
| S6-$CaCl_2$-PVP10 | 91 | 0.15 | 4.8 | – |
| S6-$CaCl_2$-PVP40 | 102 | 0.21 | 6.1 | – |

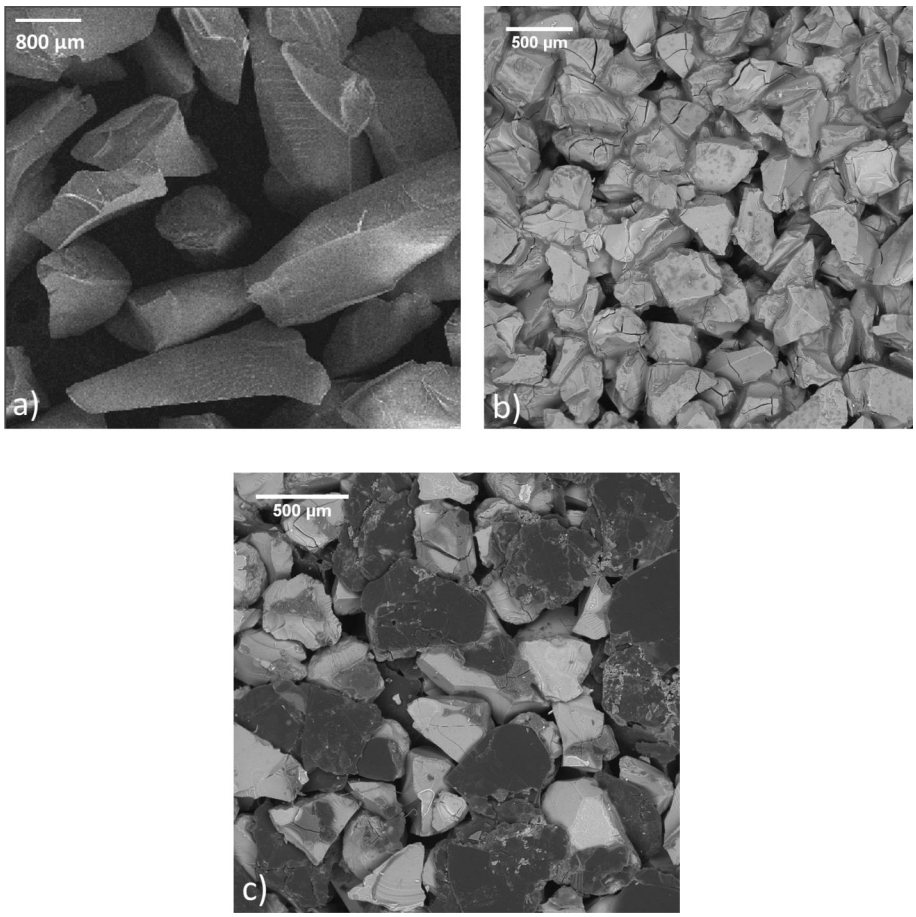


**Fig. 4.** SEM images of (a) loose grain S6 (b) S6-$CaCl_2$-PVP40 (c) S6-$CaCl_2$-PVP40-20%G.

Specific cooling performance (SCP) of both loose grains composite (S6-$CaCl_2$) and consolidated composite (S6-$CaCl_2$-PVP40) is calculated from:

$$SCP = \frac{0.8 \cdot \Delta\omega \cdot h_{fg}}{\tau_{0.8}} \quad (2)$$

where $\Delta\omega$ is total weight change, $h_{fg}$ is water enthalpy of evaporation considered 2478 kJ $kg^{-1}$ and τ is characteristic time, when time and weight changes are collected from thermogravimetric analyser with 0.2 kPa pressure step at 35 °C. The $SCP_{0.8}$ of S6-$CaCl_2$ is 55 W $kg^{-1}$, achieving 80% of its equilibrium uptake in 20 min. However, the $SCP_{0.8}$ of S6-$CaCl_2$-PVP40 is 45 W $kg^{-1}$ reaching 80% of its equilibrium uptake after 27 min. The difference in the 0.2 kPa pressure step $SCP_{0.8}$ for the samples is due to the dead weight (binder) in the S6-$CaCl_2$-PVP40 sample. For a more dramatic pressure swing, 0 to 1.2 kPa at 35 °C, the $SCP_{0.8}$ of S6-$CaCl_2$-PVP40 is 671 W $kg^{-1}$.

### 3.3. Multi-cycle performance

The large batch adsorbent composite S6-$CaCl_2$-PVP40 with 21 wt% binder was selected for cyclic testing. Fig. 9 shows pressure swing sorption cycles for S6-$CaCl_2$-PVP40. Pressure swings between 0 and 1.2 kPa at 25 and 35 °C to study the consistency of sorption performance of sorbent. In Table 5, the sorption capacity of samples at both temperatures is shown to be consistent for 150 cycles.

### 3.4. Thermal conductivity

The thermally conductivities of composite absorbents containing silica gel, PVP40% and 0–20 wt% of graphite flakes or copper powder are shown in Fig. 10. The copper powder was inhomogeneously distributed, with a greater concentration at the bottom surface of samples, while the graphite flakes were evenly dispersed in the composite absorbent. The bottom surfaces of the sample pairs tested, smooth from contact with the mold, were placed in contact with the TPS sensor. The thermal conductivity tests probed the material to a depth of 3.5 mm.

As the copper and graphite thermally conductive additives had different distributions in the composite samples, as well as different particle sizes and aspect ratios, the comparison of the thermal conductivities of the different composites is limited. However, the graphite flakes had substantially more effect on thermal conductivity than the copper powder. The thermal conductivity of the composite absorbents increased from 0.13 to 0.14 W $m^{-1}$ $K^{-1}$ as the copper powder content was increased from 0 and 20 wt%. The addition of 20 wt% graphite flakes to the composite absorbent increased the thermal conductivity from 0.13 W $m^{-1}$ $K^{-1}$ to 0.27 W $m^{-1}$ $K^{-1}$, a ~107% enhancement.

When the hygroscopic salt absorbs water vapor, it dissolves creating a liquid film inside the pores of the host silica gel. This increases the thermal conductivity and specific heat of the composite absorbent [16]. At high relative humidity, there is sharp increase in thermal conductivity associated with leakage of salt solution out of pores.

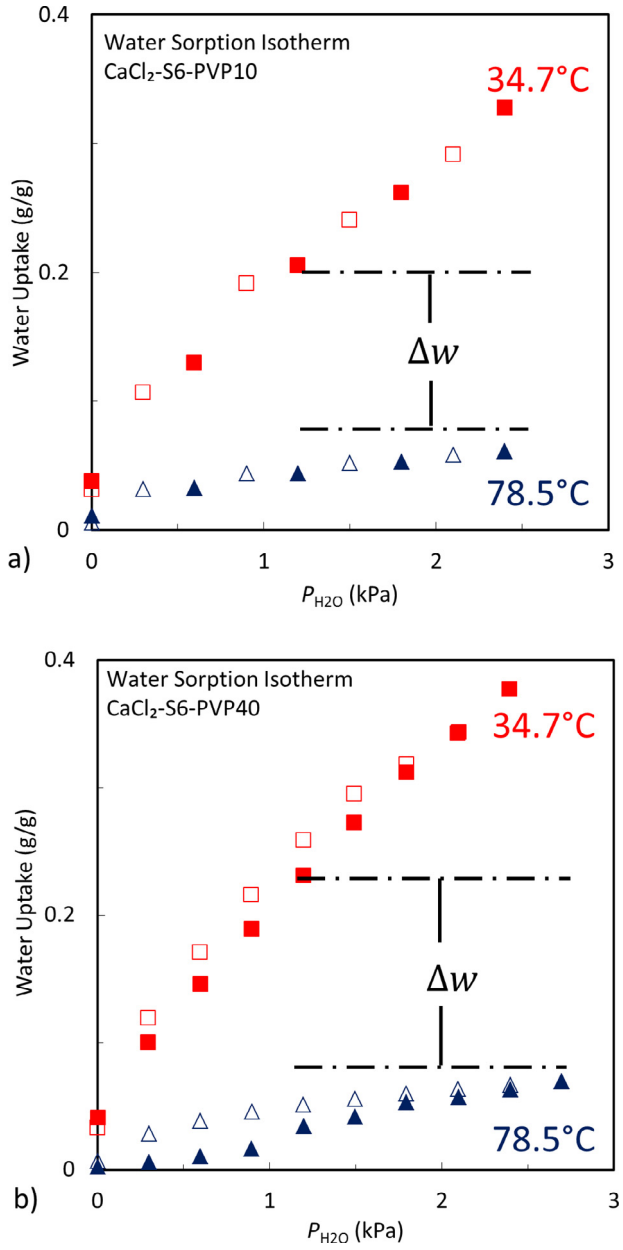


**Fig. 5.** Water uptakes with respect to pressure are shown for (a) S6-$_{CaCl2}$-PVP10 and (b) S6-$CaCl_2$-PVP40 at different temperatures 34.7 and 78.5 °C adsorption (closed symbols) and desorption (open symbols).

**Table 3**
Sorption cycle equilibrium uptake.

| Sample | $H_2O$ uptake capacity (mass%) | | $\Delta w$ (dry weight of $CaCl_2$ and silica gel only) |
|---|---|---|---|
| | 35 °C, 1.1 kPa | 80 °C, 2.3 kPa | |
| S6 | 0.54 | 0.20 | 0.34 |
| S6-$CaCl_2$ | 0.33 | 0.10 | 0.22 |
| S6-$CaCl_2$-PVP10 | 0.20 | 0.43 | 0.19 |
| S6-$CaCl_2$-PVP40 | 0.23 | 0.33 | 0.23 |

The S6-$CaCl_2$-PVP40-G sample set was tested at low RH%, 2 and 20% to evaluate the effect of water content on the thermal conductivity of the absorbent composites. As shown in Fig. 11, the increase thermal conductivity associated with the increase in

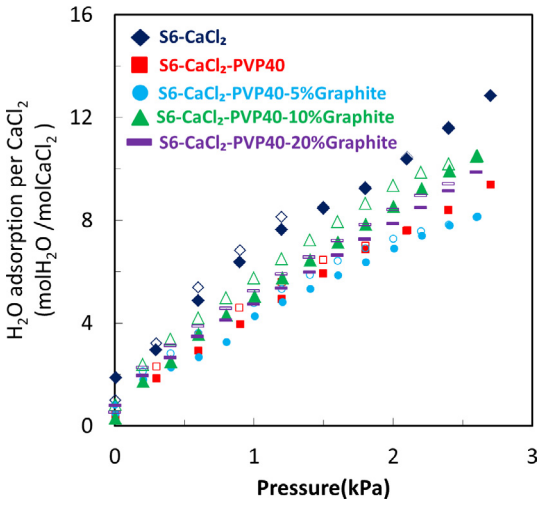


**Fig. 6.** Effect of binder and graphite flakes on water sorption capacity at 34.7 °C adsorption (closed symbols) and desorption (open symbols).

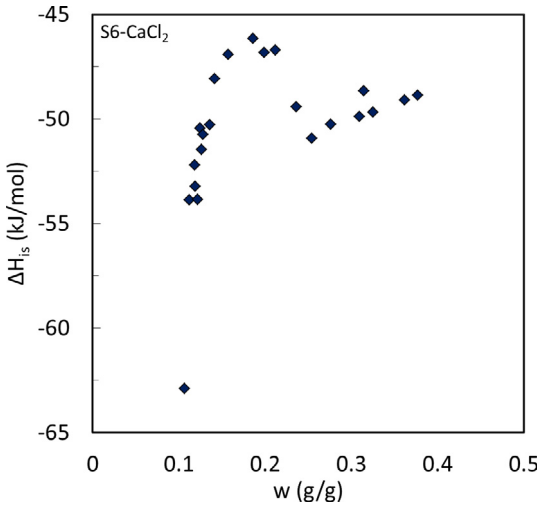


**Fig. 7.** Isosteric water sorption heat for S6-$CaCl_2$.

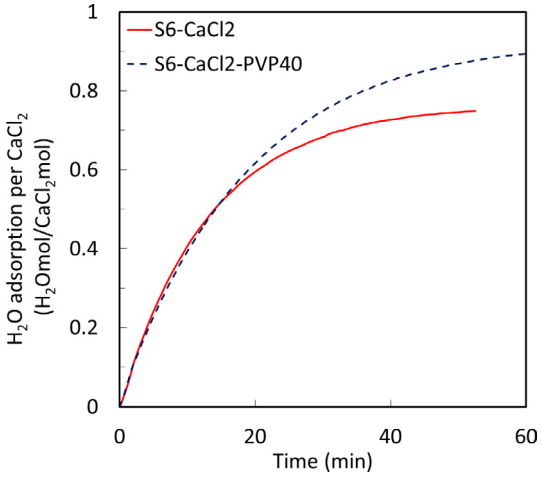


**Fig. 8.** Water vapor sorption rate of loose grain and consolidated composites containing graphite flake at 34.7 °C, 1.5 to 1.7 kPa pressure.

**Table 4**
Sorption rate coefficient of silica gel and silica-supported $CaCl_2$ composites at 35 °C.

| Sample name | Water sorption relaxation constant at 0.9–1.8 kPa vapor pressure [s] (with 0.3 kPa pressure step) | | |
|---|---|---|---|
| | 0.9 kPa | 1.2 kPa | 1.8 kPa |
| S6-$CaCl_2$ | 539 | 683 | 788 |
| S6-$CaCl_2$-PVP40 | 869 | 969 | 1090 |
| | Water sorption relaxation constant at 0.8–1.8 kPa vapor pressure [s] (with 0.2 kPa pressure step) | | |
| | 0.8 kPa | 1.2 kPa | 1.8 kPa |
| S6-$CaCl_2$-PVP40-10%G | – | 507 | 644 |
| S6-$CaCl_2$-PVP40-20%G | – | 601 | 768 |

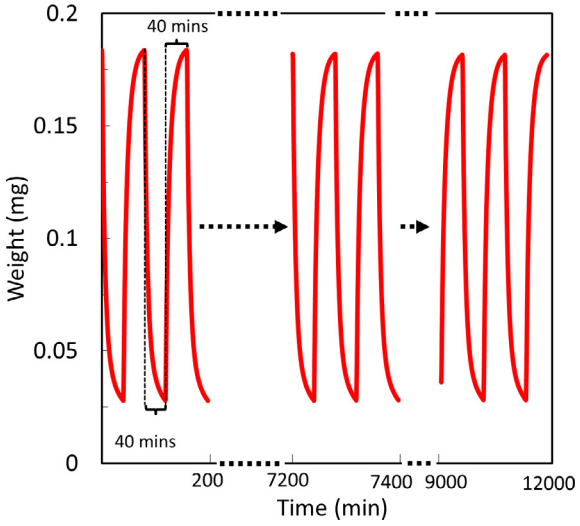


**Fig. 9.** Pressure swing (0–1.2 kPa) adsorption-desorption cycles of S6-$CaCl_2$-PVP40 at 35 °C, water uptake vs time.

**Table 5**
Multi-cycle performance of S6-$CaCl_2$-PVP40.

| *T* | Cycle number | Δ*w* (g/g) |
|---|---|---|
| 25 °C | 1 | 0.28 |
| | 10 | 0.28 |
| | 20 | 0.29 |
| | 150 | 0.29 |
| 35 °C | 160 | 0.18 |
| | 300 | 0.18 |

water content is moderate. For instance, the thermal conductivity of composite absorbent containing 10 wt% graphite flakes increased from 0.3 to 0.48 W $m^{-1}$ $K^{-1}$ as its equilibrium water content increased from 0.06 g/g and 0.19 g/g, for 2 and 20%RH test conditions, respectively.

## 4. Conclusion

New composite adsorbents were prepared by consolidating graphite flakes with silica gel using binders with different molecular weights, and their water uptake capacities measured at different partial pressures. The effect of thermally conductive additives on water uptake and thermal conductivity studied.

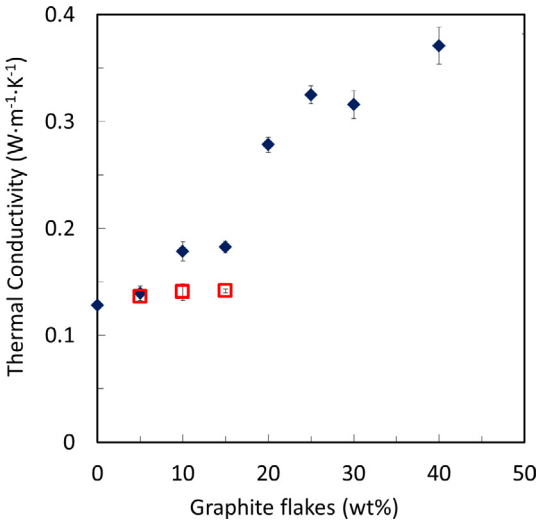


**Fig. 10.** Thermal conductivity of silica gel consolidated with 15 wt% PVP40 binder and 0–50 wt% of either graphite flakes (◆) and copper powder (□).

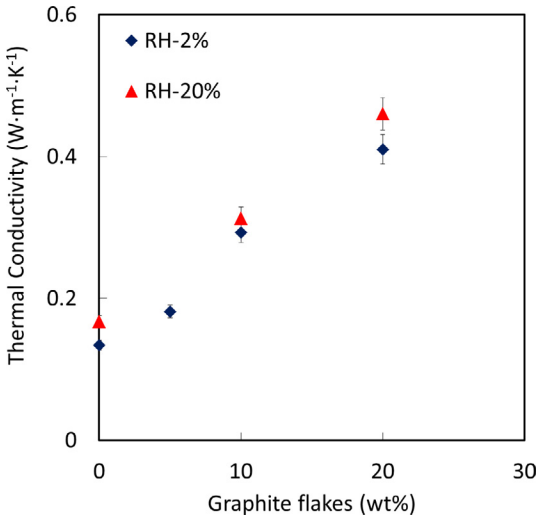


**Fig. 11.** Thermal conductivity of consolidated composite sorbents (S6-$CaCl_2$ PVP40-0%, 5%, 10% and 20% G) with 0–20 wt% graphite flakes at 2 and 20 RH%.

- The 40,000 MW PVP binder had substantially less effect on the pore volume, pore size distribution and water uptake of silica gel-$CaCl_2$ composites than the 10,000 MW PVP binder.
- The water uptake of the silica gel-$CaCl_2$-PVP40 composite was consistent through 300 pressure swing cycles.
- The thermal conductivity of a set of S6-$CaCl_2$–PVP40 sorbent with 0–20 wt% graphite flakes were tested at 2 and 20 RH%. The absorbed water at 20 RH% increased the thermal conductivity of the sample by 0.13–0.16 W $m^{-1}$ $K^{-1}$.

A gravimetric test apparatus is currently being used to evaluate the performance of consolidated sorbent on small heat exchanger components. Consolidated adsorbent with greater salt content will be synthesized and characterized.

## Acknowledgments

The authors gratefully acknowledge the financial support of the Natural Sciences and Engineering Research Council of Canada (NSERC) through Automotive Partnership Canada Grant No. APCPJ

429698-1 and Pacific Institute for Climate Solutions (PICS) graduate fellowship. We thank Dr. D. Leznoff and Mr. Ryan Roberts for their assistance with nitrogen adsorption experiments. The SEM studies were conducted in the Simon Fraser University 4D Labs facility with the assistance of the technical staff. 4D LABS shared facilities are supported by the Canada Foundation for Innovation (CFI), British Columbia Knowledge Development Fund (BCKDF), Western Economic Diversification Canada (WD), and Simon Fraser University (SFU).

## References

[1] R.E. Critoph, Solid sorption cycles: a short history, Int. J. Refrig. 35 (3) (2012) 490–493.
[2] E.B. Miller, The development of silica gel refrigeration, Refrig. Eng. 17 (4) (1929) 103–108.
[3] G.E. Hulse, Freight car refrigeration by an adsorption system employing silica gel, Refrig. Eng. 17 (1929) 41–54.
[4] R.E. Critoph, Y. Zhong, Review of trends in solid sorption refrigeration and heat pumping technology, Proc. Inst. Mech. Eng. Part E J. Process Mech. Eng. 219 (3) (2005) 285–300.
[5] Y.I. Aristov, Current progress in adsorption technologies for low-energy buildings, Future Cities Environ. 1 (1) (2015) 10.
[6] A. Jabbari-Hichri, S. Bennici, A. Auroux, Enhancing the heat storage density of silica alumina by addition of hygroscopic salts ($CaCl_2$, $Ba(OH)_2$, and $LiNO_3$), Sol. Energy Mater. Sol. Cells 140 (2015) 351–360.
[7] A.N. Shmroukh, A.H.H. Ali, S. Ookawara, Adsorption working pairs for adsorption cooling chillers: a review based on adsorption capacity and environmental impact, Renew. Sustain. Energy Rev. 50 (2015) 445–456.
[8] A. Sharafian, K. Fayazmanesh, C. McCague, M. Bahrami, Thermal conductivity and contact resistance of mesoporous silica gel adsorbents bound with polyvinylpyrrolidone in contact with a metallic substrate for adsorption cooling system applications, Int. J. Heat Mass Transf. 79 (2014) 64–71.
[9] S.G. Wang, R.Z. Wang, X.R. Li, Research and development of consolidated adsorbent for adsorption systems, Renew. Energy 30 (9) (Jul. 2005) 1425–1441.
[10] A. Rezk, R.K. Al-Dadah, S. Mahmoud, A. Elsayed, Effects of contact resistance and metal additives in finned-tube adsorbent beds on the performance of silica gel/water adsorption chiller, Appl. Therm. Eng. 53 (2) (2012) 278–284.
[11] A. Freni, A. Sapienza, I.S. Glaznev, Y.I. Aristov, G. Restuccia, Experimental testing of a lab-scale adsorption chiller using a novel selective water sorbent 'silica modified by calcium nitrate', Int. J. Refrig. 35 (3) (May 2012) 518–524.
[12] I.V. Ponomarenko, I.S. Glaznev, A.V. Gubar, Y.I. Aristov, S.D. Kirik, Synthesis and water sorption properties of a new composite '$CaCl_2$ confined into SBA-15 pores', Micropor. Mesopor. Mater. 129 (1–2) (2010) 243–250.
[13] I. Glaznev, I. Ponomarenko, S. Kirik, Y. Aristov, Composites $CaCl_2$/SBA-15 for adsorptive transformation of low temperature heat: Pore size effect, Int. J. Refrig. 34 (5) (2011) 1244–1250.
[14] Y.I. Aristov, New family of solid sorbents for adsorptive cooling: material scientist approach, J. Eng. Thermophys. 16 (2) (2007) 63–72.
[15] A. Freni, G. Maggio, A. Sapienza, A. Frazzica, G. Restuccia, S. Vasta, Comparative analysis of promising adsorbent/adsorbate pairs for adsorptive heat pumping, air conditioning and refrigeration, Appl. Therm. Eng. 104 (2016) 85–95.
[16] Y.Y. Tanashev, A.V. Krainov, Y.I. Aristov, Thermal conductivity of composite sorbents 'salt in porous matrix' for heat storage and transformation, Appl. Therm. Eng. 61 (2) (2013) 401–407.
[17] A. Freni, A. Frazzica, B. Dawoud, S. Chmielewski, L. Calabrese, L. Bonaccorsi, Adsorbent coatings for heat pumping applications: Verification of hydrothermal and mechanical stabilities, Appl. Therm. Eng. 50 (2) (2013) 1658–1663.
[18] M. Tatlier, G. Munz, G. Fueldner, S.K. Henninger, Effect of zeolite A coating thickness on adsorption kinetics for heat pump applications, Micropor. Mesopor. Mater. 193 (2014) 115–121.
[19] L. Pino, Y.U. Aristov, G. Cacciola, G. Restuccia, Composite materials based on zeolite 4A for adsorption heat pumps, Adsorption 40 (1997) 33–40.
[20] C.-H. Wu, S.-H. Hsu, R.Q. Chu, M.-T. Chen, T.-W. Chung, Enhancing the thermal conductivity of the heat exchanger in a noncompressive system as a means of energy efficiency improvement of the system, Int. J. Green Energy 6 (2014) (2009) 490–507.
[21] H. Demir, M. Mobedi, S. Ülkü, The use of metal piece additives to enhance heat transfer rate through an unconsolidated adsorbent bed, Int. J. Refrig. 33 (2010) 714–720.
[22] T. Eun, H. Song, J. Hun, K. Lee, J. Kim, Enhancement of heat and mass transfer in silica-expanded graphite composite blocks for adsorption heat pumps: Part I. Characterization of the composite blocks, Int. J. Refrig. 23 (2000) 64–73.
[23] T. Eun, H. Song, J. Hun, K. Lee, J. Kim, Enhancement of heat and mass transfer in silica-expanded graphite composite blocks for adsorption heat pumps. Part II. Cooling system using the composite blocks, Int. J. Refrig. 23 (2000) 74–81.
[24] P.P. Barrett, E.P. Joyner, L.G. Halenda, The determination of pore volume and area distributions in porous substances, computations from nitrogen isotherms, J. Am. Chem. Soc. 73 (1951) 373–380.
[25] W. Bauer, J. Herrmann, R. Mittelbach, W. Schwieger, Zeolite/aluminum composite adsorbents for application in adsorption refrigeration, Int. J. Energy Res. 33 (2009) 1233–1249.
[26] S.A. Al-Ajlan, Measurements of thermal properties of insulation materials by using transient plane source technique, Appl. Therm. Eng. 26 (17–18) (2006) 2184–2191.
[27] S.E. Gustafsson, Transient plane source techniques for thermal conductivity and thermal diffusivity measurements of solid materials, Rev. Sci. Instrum. 62 (3) (1991) 797–804.
[28] Y. He, Rapid thermal conductivity measurement with a hot disk sensor: Part 1. Theoretical considerations, Thermochim. Acta 436 (1–2) (2005) 122–129.
[29] S. Santamaria, A. Sapienza, A. Frazzica, A. Freni, I.S. Girnik, Y.I. Aristov, Water adsorption dynamics on representative pieces of real adsorbers for adsorptive chillers, Appl. Energy 134 (2014) 11–19.